Mixed Convection in The Entry Region of a Vertical Annulus with a Constant Temperature Rotating Inner Cylinder

Akeel A. Mohammed

Received on: 15/3/2005
Accepted on: 18/7/2005

Abstract

Laminar air flow combined convection in a vertical annulus with a constant temperature rotating inner cylinder is treated on the basis of a developing flow model, and the basic differential equations are rewritten in finite difference form and solved by a computer program in Fortran. Investigation covers the ranges of $0.2 \le N \le 0.9$, $-300 \le Gr/Re \le 800$ and $0.2 \le Re^2/Ta \le 1000$. In addition to the usual heat transfer calculations, this enables the developing velocity and temperature fields to be studied. On the other hand , the effect of a superimposed aiding or opposing natural convection on the developing tangential velocity profile is also investigated.

الحمل المختلط في مدخل تجويف حلقي عمودي ذو أسطوانة داخلية دوارة ذات درجة حرارة ثابتة

الخلاصة

الحمل المركب لتدفق الهواء الطباقي بتجويف حلقي عمودي و بأسطوانة داخلية دوّارة ذات درجة حرارة ثابتة يعامل على مبدأ نموذج جريان التشكيل ، و تعاد كتابة المعادلات التفاضلية الأساسية على شكل فروقات محددة و تُحل باستخدام برنامج حاسوبي بلغة فورتران. التحري يغطي المديات $0.2 \le N \le 0.9$, $-300 \le Gr/Re \le 800$, $0.2 \le Re^2/Ta \le 1000$ بالإضافة إلى حسابات انتقال الحرارة المفيدة ، فأن ذلك يمكّن مجالات سرعة و درجة حرارة التشكيل لتكون مدروسة. على الجانب الآخر فقد تم التحري عن تأثير الحمل الحر المساعد أو المتعاكس الإضافي على منحى التشكيل للسرعة المماسية.

Nomenclature

b, annular gap width , (r_2-r_1) ;
c, specific heat of fluid at constant pressure ;
D_h'{, hydraulic diameter of annulus, 2b ;
g , gravitational body force per unit mass ;
Gr, modified Grashof number , $g\rho\beta(t_w-t_i)D_h^3/\nu^2$;
h , local heat transfer coefficient based on area of heated surface , $k\ \partial t/\partial r\ /(t_w-t_m)$;
L , annulus length ;
k , thermal conductivity of fluid ;
n, number of radial increaments in the numerical mesh network ;
N, annulus radius ratio ,r_1/r_2 ;
Nu, local Nusselt number ;
p , pressure of fluid at any point ;
p_i , pressure of fluid at annulus entrance ;
p_s , hydrostatic pressure , $\pm \rho_i g z$;
$\bar{p}$, pressure defect at any point , $p-p_s$;

https://doi.org/10.30684/etj.25.1.9
2412-0758/University of Technology-Iraq, Baghdad, Iraq

P, dimensionless pressure defect at any point , $(\bar{p}-p_i)/\rho_i u_i^2$;
Pr, Prandtl number , $\mu c/k$;
r, radial coordinate ;
r_1, inner radius ;
r_2, outer radius ;
R, dimensionless radial coordinate , r/r_2 ;
Re , Reynolds number , $u_i D/\nu$;

RR, dimensionless radial coordinate , $r-r_1/r_2-r_1$;
t , fluid temperature ;
t_m, mixing cup temperature over any cross-section ,
$\int_{r_1}^{r_2} u\, t\, r\, dr \Big/ \int_{r_1}^{r_2} u\, r\, dr$;
t_i , fluid temperature at annulus entrance ;
T, dimensionless temperature , $(t-t_i)/(t_w-t_i)$;
T_m , dimensionless mixing cup temperature , $(t_m-t_i)/(t_w-t_i)$;
T_a, Taylor number , $2\Omega^2 r_1^2 b^3/\nu^2(r_1+r_2)$;
u , axial velocity ;
u_i , entrance axial velocity , $\int_{r_1}^{r_2} ur\, dr \Big/ \int_{r_1}^{r_2} r\, dr$;
U, dimensionless axial velocity , u/u_i ;
v , radial velocity ;
V, dimensionless radial velocity , $v\, r_2/\nu$;
w , tangential velocity ;
W, dimensionless tangential velocity , $w/\Omega\, r_1$;
z , axial coordinate ;
Z, dimensionless axial coordinate , $2z(1-N)/r_2\, Re$

Greek symbols

β , volumetric coefficient of thermal expansion ;
ρ , fluid density , $\rho_i [1-\beta(t-t_i)]$;
ρ_i , fluid density at the entrance temperature ;
μ , dynamic viscosity of fluid ;
ν , kinematic viscosity of fluid ;
Ω , angular velocity of inner cylinder.

1. Introduction

Combined (or mixed) convection arises when the normal modes of convection , viz. natural and forced, are simultaneously present. This problem is complex because of the large number of interacting parameters, including the relative direction of the natural and forced convections, the geometry of arrangement, the flow condition, and the boundary conditions.

The investigating of laminar mixed convection in an annulus with the rotating inner cylinder leads to a basic understanding of a fluid flow through the gap between rotating and stationary machine parts and improving the design of such equipment and hence minimize possible failures. The vertical electric machines are an example of such equipment in which the heat resulting from the iron and copper losses is conducted to the rotor surface where it is transferred to the air in the annular gap between the rotor and the stator. Therefore, the design of cooling systems for such types of electric machines in which heat is transferred by natural convection and radiation requires a knowledge of the hydrodynamic behavior of the free convection flow to limit the rotor temperature to less than the maximum permitted value. Besides other

applications in chemical mixing process, swirl nozzles, combustion chambers, fiber coating applications and dry machinary [١], gas or oil exploration drills, journal bearing [٢], rotating heat exchangers, atmospheric circulation [٧], cooling of rotor blades of gas-turbines, ramjets attached to the rotors of helicopters , rotating condensers for sea water distillation [٨], and so on.

Few papers in the literature [1-8] have dealt with tangentially developing laminar flows and/or transition to vorticular motion in the entrance region of concentric annuli with rotating inner walls. The main aim of these papers was the determination of the axial growth of the tangential boundary layer displacement thickness. In fact, most of these entry region investigations have been developed under the assumption of temperature independent fluid properties. However high heating or cooling rates may cause significant changes in fluid properties and the classical assumption of constant physical properties may lead to considerable errors in predicting the flow behavior and both the power required to pump the fluid and heat transfer characteristics. Hessami, et.al [5], presented a numerical study for the laminar flow patterns and heat transfer for air contained in the enclosure formed between two vertical, concentric cylinders and two horizontal planes. The inner cylinder and one of the horizontal planes were heated and rotated about the vertical axis; the other horizontal plane and outer cylinder were cooled and kept stationary. Solutions obtained for $1.2 \le r_2/r_1 \le 8$, $10 \le Re \le 300$ and $10^3 \le Ra \le 10^5$. The influences of geometry, Ra and Re on temperature and velocity distributions were investigated. El-Shaarawi and Sarhan [2] , performed numerical results of a finite difference scheme for the developing mixed laminar boundary layer flow in a concentric annulus of 0.9 radius ratio with a rotating inner cylinder under the thermal conditions of one wall being isothermal and the opposite wall adiabatic. The study covered the ranges of $-300 \le Gr/Re \le 800$ and $0.2 \le Re^2/Ta \le 10$. The effects of a rotating inner cylinder on the hydrodynamic development length , critical distance at which the axial velocity gradient normal to the wall vanishes and heat transfer parameters were also considered. Ho and Tu [7] , made a numerical investigation to evaluate the perturbing effect of forced convection due to axial rotating of the inner cylinder on natural convection heat transfer of cold water with density inversion effects in a cylindrical annulus of 2 radius ratio and ranges of $10 \le Re \le 200$, and $10^3 \le Ra \le 10^6$. The mixed convection heat and fluid flow structures in the annulus were found to be strongly affected by the density inversion effects.

The present study is an attempt to investigate the free convection effects on the developing laminar upward or downward flow in a vertical annulus with a constant temperature rotating inner cylinder and adiabatically insulated stationary outer cylinder.

2. Governing Equations

Assuming steady, axisymmetric , laminar flow of an incompressible

Newtonian fluid, with no internal heat generation, with constant physical properties except the density which only varies in the gravitational body force term according to the Boussinesq approximation , neglecting viscous dissipation and axial conduction of heat , assuming Re>>0 , and applying the Prandtl boundary layer assumptions [2], the equations governing the mixed convection in the entrance region of a vertical annulus with a rotating inner cylinder are as follows:

$$\frac{\partial(rv)}{\partial r}+\frac{\partial(ru)}{\partial z}=0 \qquad \text{……..(1)}$$

$$\rho_i\frac{w^2}{r}=\frac{\partial p}{\partial r} \quad , \quad \text{…….(2)}$$

$$\rho_i\left(v\frac{\partial w}{\partial r}+u\frac{\partial w}{\partial z}\right)=\mu\frac{\partial}{\partial r}\left[\frac{1}{r}\frac{\partial}{\partial r}(rw)\right]$$

$$\text{……..(3)}$$

$$\rho_i\left(v\frac{\partial u}{\partial r}+u\frac{\partial u}{\partial z}\right)=-\frac{\partial p}{\partial z}\mp\rho_i g\left[1-\beta\left(t-t_i\right)\right]+\frac{\mu}{r}\frac{\partial}{\partial r}\left(r\frac{\partial u}{\partial r}\right)$$

$$\text{……(4)}$$

$$\rho_i c\left(v\frac{\partial t}{\partial r}+u\frac{\partial t}{\partial z}\right)=\frac{k}{r}\frac{\partial}{\partial r}\left(r\frac{\partial t}{\partial r}\right)$$

$$\text{.....…..(5)}$$

The minus and plus signs in the gravitational term of equation(4) apply respectively to upward and downward flows, taking into consideration that the force acts in the negative z-direction in case of an upward flow and vice versa in case of a downward flow.

Dissociating the pressure into the usual two component, i.e.

$$p=\bar{p}+p_s=\bar{p}\mp\rho_i g\mathbf{Z} \qquad \text{,……(6)}$$

in which the minus and plus signs apply respectively to upward and downward flows, equations (2) and (4) can be written as follows

$$\rho_i\frac{w^2}{r}=\frac{\partial\bar{p}}{\partial r} \quad , \text{……(7)}$$

$$\rho_i\left(v\frac{\partial u}{\partial r}+u\frac{\partial u}{\partial z}\right)=-\frac{\partial\bar{p}}{\partial z}\pm\rho_i g\beta\left(t-t_i\right)+\frac{\mu}{r}\frac{\partial}{\partial r}\left(r\frac{\partial u}{\partial r}\right) \qquad \text{.....……..(8)}$$

Using the dimensionless parameters given in the nomenclature, equations (1), (3), (5), (7) and (8) can be replaced by the following dimensionless forms:

$$\frac{\partial V}{\partial R}+\frac{V}{R}+\frac{\partial U}{\partial Z}=0 \qquad \text{……(9)}$$

$$\frac{W^2}{R}=\frac{(1-N)}{2(1+N)}\frac{Re^2}{Ta}\frac{\partial P}{\partial R} \qquad \text{…..(10)}$$

$$V\frac{\partial W}{\partial R}+U\frac{\partial W}{\partial Z}=\frac{\partial^2 W}{\partial R^2}+\frac{1}{R}\frac{\partial W}{\partial R}-\frac{W}{R^2}$$

$$\text{……(11)}$$

$$V\frac{\partial U}{\partial R}+U\frac{\partial U}{\partial Z}=-\frac{\partial P}{\partial Z}\pm\frac{Gr}{Re}\frac{T}{4(1-N)^2}+\frac{\partial^2 U}{\partial R^2}+\frac{1}{R}\frac{\partial U}{\partial R} \qquad \text{..……(12)}$$

$$V\frac{\partial T}{\partial R}+U\frac{\partial T}{\partial Z}=\frac{1}{Pr}\left(\frac{\partial^2 T}{\partial R^2}+\frac{1}{R}\frac{\partial T}{\partial R}\right)$$

$$\text{…….(13)}$$

The five coupled equations (9)-(13) are subjected to the following boundary conditions:

1. For $Z \geq 0$ and $R=N$,
   $U=V=0, W=1, T=1$

2. For $Z \geq 0$ and $R=1$,
   $U=V=W=0$, $\partial T/\partial R=0$

3 .For $Z=0$,
   $U=1$, $V=W=0$, $P=0$, $T=0$

The integral continuity equation can be written in the form :

$$\int_N^1 RU \; dR = \frac{1}{2}\left(1 - N^2\right) \quad \text{.....(15)}$$

3. Numerical Solution

Considering the mesh net work of Fig.(1), and an extension of the work of [2], equations (9)-(13) and equation (15) can be written in the following finite difference forms:

$$\frac{V_{i+1,j+1} - V_{i,j+1}}{\Delta R} + \frac{V_{i+1,j+1} + V_{i,j+1}}{2\left[N + (i-1)\Delta R\right]} + \frac{U_{i+1,j+1} + U_{i,j+1} - U_{i+1,j} - U_{i,j}}{2\Delta Z} = 0$$

.....(16)

$$V_{i,j}\frac{U_{i+1,j+1} - U_{i-1,j+1}}{2\Delta R} + U_{i,j}\frac{U_{i,j+1} - U_{i,j}}{\Delta Z} = \frac{P_{i,j} - P_{i,j+1}}{\Delta Z} + \frac{Gr}{4Re(1-N)^2}T_{i,j+1}$$

$$+ \frac{U_{i+1,j+1} - 2U_{i,j+1} + U_{i-1,j+1}}{\Delta R^2} + \frac{1}{N + (i-1)\Delta R}\frac{U_{i+1,j+1} - U_{i-1,j+1}}{2\Delta R}$$

.....(17)

$$\frac{W_{i,j}W_{i,j+1}}{N + (i-1)\Delta R} = \frac{(1-N)}{2(1+N)}\frac{Re^2}{Ta}\frac{P_{i,j+1} - P_{i-1,j+1}}{\Delta R} \quad \text{.....(18)}$$

$$V_{i,j}\frac{W_{i+1,j+1} + W_{i+1,j} - W_{i-1,j} - W_{i-1,j+1}}{4\Delta R} + U_{i,j}\frac{W_{i,j+1} - W_{i,j}}{\Delta Z} =$$

$$-\frac{W_{i,j+1} + W_{i,j}}{2\left[N + (i-1)\Delta R\right]^2} + \frac{1}{N + (i-1)\Delta R}\frac{W_{i+1,j+1} + W_{i+1,j} - W_{i-1,j} - W_{i-1,j+1}}{4\Delta R}$$

$$+ \frac{W_{i+1,j+1} + W_{i+1,j} - 2W_{i,j+1} - 2W_{i,j} + W_{i-1,j+1} + W_{i-1,j}}{2(\Delta R)^2} \quad \text{.....(19)}$$

$$V_{i,j}\frac{T_{i+1,j+1}-T_{i-1,j+1}}{2\Delta R}+U_{i,j}\frac{T_{i,j+1}-T_{i,j}}{\Delta Z}=+\frac{1}{N+(i-1)\Delta R}\frac{T_{i+1,j+1}-T_{i-1,j+1}}{2\Delta R}+\frac{1}{Pr}\frac{\left(T_{i+1,j+1}-2T_{i,j+1}+T_{i-1,j+1}\right)}{(\Delta R)^2}\ldots\ldots\ldots(20)$$

$$\Delta R\sum_{i=2}^{n}U_{i,j}\left[N+(i-1)\Delta R\right]=\frac{1}{2}\left(1-N^2\right)\qquad\ldots\ldots\ldots\ldots(21)$$

In the above finite difference equations the variables with subscript j+1 represent the unknowns and those with subscript j are known. The numerical solution of these equations is obtained by first selecting values of the parameters Re^2/Ta , Gr /Re and Pr. Then , starting with j=1 (entrance cross-section) and applying equation (19) for i=2,3,…..,n yields (n-1) simultaneous linear algebraic equations which when solved by Gauss-Siedel elimination method give the unknown values of W's at all points of the second cross-section. Similarly , using equation (20) the unknown values of T's at all points of the second cross-section (j=2) are obtained. Now, applying (18) with j=2,3,…..,n+1 and (17) with i=2,3,….,n and (21) to the entire cross-section, we get 2n equations which when solved, by means of a special form of the Gauss-Siedel elimination scheme , give the unknown values of U's and P's at all points of the second cross-section. Using the computed values of U's and applying (16) we get the unknown values of V's at the grid points of the second cross-section. Repeating this procedure, we can advance along the annulus until the flow becomes fully developed.

Knowing the temperature profiles from numerical solution of energy, the mixing cup temperature and the local Nusselt number at any cross-section can be calculated.

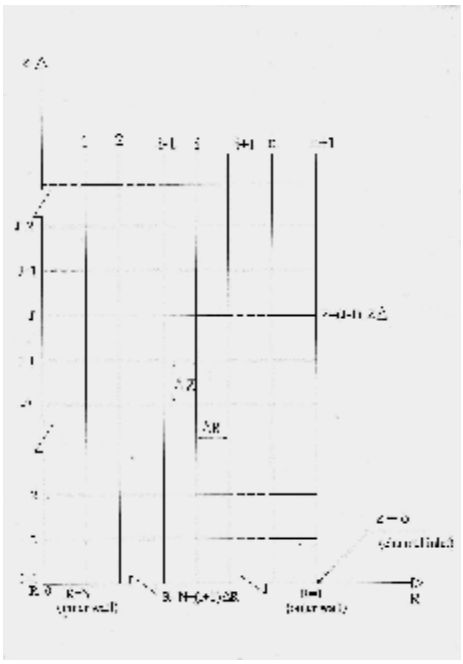

Fig.(1) Mesh network of finite difference representation

Results and Discussion

4.1 Velocity Profile

Development axial velocity profiles along the vertical annulus axis with the rotating inner cylinder are shown in Figs.(٢-١٠). Fig.(2) and Fig.(3) show the development of the axial velocity profile, for N=0.9, Re^2/Ta=10, and Gr/Re=200 &800 respectively. It is clear from these two figures that when the free convection aids the forced flow (i.e., positive Gr/Re for heating with up flow or cooling with down flow) the fluid accelerates near the heated boundary and decelerates near the opposite insulated wall. The developing axial velocity profiles deviate increasingly from the corresponding isothermal (or constant density) profiles until a cross-section of a maximum velocity distortion, at which the slop of the profile ($\partial U/\partial R$) at the insulated wall becomes a minimum is reached. As the axial distance increases further, the axial velocity profile recovers and approaches the fully developed isothermal profile as the fluid temperature approaches the isothermal wall temperature. This behavior is more pronounced in Fig.(3) than Fig.(2) in which the maximum velocity upstream bias toward the annular gap core because of the dominant forced convection in the heat transfer process. This behavior can be physically explained as follows: consider the air in the annular gap at some arbitrary location and let $t_w > t_b$. The temperature of the air must decrease in the radial direction, this leads to increasing the air density with R. Therefore; the declarative effect of gravitational body force, which is proportional to the density, increases in the radial direction. As a result, the air will tend to rise more rapidly in the axial direction near the heated wall and tends to slow up toward outer wall. There is a non-significant effect of Re^2/Ta on the developing velocity profile because of the highly Re comparison with Ta (Re^2/Ta=10).

Figs.(٤&5) show the effect of the parameter Gr/Re on the axial velocity profile for N=0.9 & 0.555 ; Re^2/Ta=10 & ∞ and at Z=0.0008 & 0.004 respectively. It is clear from these two figures that, when the free convection opposes the forced flow (i.e., negative Gr/Re for heating with down flow or cooling with up flow) the buoyancy force tends to retard the fluid near the heated boundary and accelerates it near

the opposite adiabatic wall. In such a case the maximum velocity profile distortion occurs when the slop of the profile at the heat transfer boundary reaches its minimum value. Therefore; in this case a possibility of flow reversal may occur near the heated wall if the natural convection is opposing the forced flow. On the other hand, and as be explained before, when the free convection aids the forced flow (i.e., upward flow) the fluid accelerates near the heated wall and decelerates near the opposite adiabatic boundary. In the present analysis, the same velocity profile characterized is presented by El-Shaarawi and Sarhan [2].

In the case of Gr/Re=0 (pure forced convection) the maximum velocity occurs at the annular gap centerline (fully developed velocity profile) and the hydrodynamic development length increases as the inner cylinder rotation increases in comparison with the case of flow in a stationary annulus (i.e., $Re^2/Ta= \infty$). This increase in the hydrodynamic development length is dependent on the values of parameter Re^2/Ta.

Fig.(٦) and Fig.(٧) show the effect of radius ratio on the axial velocity profile for Gr/Re=500 (aiding flow), $Re^2/Ta=0.2$ (i.e., the lowest value at which a converged laminar solution could be obtained over the entire development length for the selected value of Gr/Re), and at Z=0.0002 (upstream) and Z=0.002 (downstream), respectively. It is obvious from Fig.(٦) that at the entrance , the axial velocity profile seems more uniform in the region of RR bounded between 0.1 and 0.8 for the first three curves (i.e., N≤0.7) and deviates increasingly toward the heated surface for N=0.9 and reaches a maximum value at RR=0.25. It is clear that , the axial velocity increases as the radius ratio of annulus increases (i.e., the cross-sectional area of the annular gap decreases); leads to increasing of the amount of heat per unit volume inside the annular gap (i.e., increasing of natural convection). As a result, the fluid will accelerate near the heated wall and decelerates near the outer wall.

This behavior will continue downstream as shown in Fig.(٧). The axial velocity profiles begin to be developed as the flow progresses further downstream by biasing the maximum axial velocity firstly toward the heated surface. This behavior is more obviously in Fig.(٨) which shows the effect of radius ratio on the axial velocity profiles for Gr/Re=500, $Re^2/Ta=10$ (i.e., slow rotational velocity of the inner cylinder) and at Z=0.004 (downstream).

Fig.(9) reveals the effect of radius ratio the axial velocity profiles for Gr/Re=0 (i.e., pure forced convection), $Re^2/Ta=0.2$ and at Z=0.0004. It is clear from this figure that there is non-significant effect for rotational velocity of the inner wall on behavior of the velocity profiles that the upper half of the axial velocity profiles across the annular gap is slightly differ from that in lower half, and the flow seems more developed in the last curve (N=0.9) from these in the 1st three curves (N=0.2, 0.55, and 0.7) which appear more

uniformly in the region of RR bounded between 0.15 and 0.8.

The same behavior of the axial velocity profiles as in Fig.(9) will be obtained for the same input conditions except Gr/Re= –300 (i.e., opposing flow) as shown in Fig.(١٠). It is noticed from this figure that the maximum axial velocity in the last curve (N=0.9) bias towards the outer wall and seems more developed than the 1st three curves (N=0.3, 0.55, and 0.7) which seem more uniformly in the region of RR bounded between 0.15 and 0.8.

4.2 Temperature Profile

The developing of temperature profiles along the vertical annulus with a rotating inner cylinder , are shown in Fig.(١١) and Fig.(١٢) which represent N=0.555, Gr/Re=500 (aiding flow), Re^2/Ta=0.2 (i.e., high rotational velocity of the inner cylinder) and 10 (i.e., very slow rotational velocity of the inner cylinder) respectively. It is evident from these two figures that no significant effect of the rotational velocity of the inner cylinder on the heat transfer process. It is clear also from these two figures that there is a steep temperature gradient near the heated wall due to the natural convection effects and no appreciable temperature variations in the region bounded between the annulus gap core and the outer wall due to poverty of natural convection in this region. It is noticed also that the thickness of the thermal boundary layer gradually increases as the flow moves from annulus inlet toward annulus exit.

Fig.(١٣) shows the effect of the parameter Gr/Re (i.e., natural convection term) on the developing of temperature profile for N=0.9, Re^2/Ta=10, and at Z=0.008. It is noticeable from this figure that, the corresponding temperature values for each value of Gr/Re at the same R (or the temperature profile development) decreases as the aiding free convection increases (i.e., positive values of Gr/Re) and vice versa for the opposing free convection (i.e., negative values of Gr/Re). The case of a pure forced convection (i.e., Gr/Re=0) lies between them. It can be clearly seen that as the positive parameter Gr/Re increases as the wall-mixing cup temperature difference decreases and an improving the heat transfer process will be obtained.

This behavior will change as shown in Fig.(١٤) & Fig.(١٥) which represent the effect of the parameter Gr/Re on the developing temperature profiles for N=0.555 , (Re^2/Ta=0.2, Z=0.001) and (Re^2/Ta=10, Z=0.0008) , respectively. It can be seen that no appreciable effect of an increasing the natural convection (i.e., increasing of Gr/Re) in both cases: aiding and opposing flows (i.e., positive and negative values of Gr/Re, respectively) on the developing temperature profiles because of the dominant forced convection in the heat transfer process when the radius ratio decreases from 0.9 to 0.555.

Fig.(١٦) shows the effect of radius ratio on the developing temperature profile for Gr/Re=500, Re^2/Ta=0.2, and at Z=0.0002

(upstream). It is evident that there is no temperature variation in the 1st three curves corresponding to the radius ratio's 0f 0.3, 0.555, and 0.7 in the region bounded between RR=0.25 and RR=1 (i.e., outer wall). On the other hand, there is a very steep temperature gradient near the heated wall and the values of temperature in this region increase as the radius ratio increases. This behavior can be attributed to the fact that says, as the radius ratio increases, the gap in the annulus would be small leading to implying more efficient heating for this case (i.e., the heat transfer process in small radius ratio is better than that in higher radius ratio).

The temperature profiles will be more developing downstream (Z=0.002) for the same values of Gr/Re & Re^2/Ta and for the corresponding values of radius ratio as shown in Fig.(١7). This can be attributed to approaching the fully developed isothermal temperature profile which increases in the aiding flow case and decreases in the opposing flow case.

Fig.(١8) represents the effect of radius ratio on the developing temperature profiles for Gr/Re=0 (i.e., pure forced convection) , Re^2/Ta=0.2, and at Z=0.0004. It can be seen that the same tendency as that of Fig.(١6) has been approximately obtained. The temperature profile will be more developed as the radius ratio increases (i.e., annular gap decreasing) because of the dominating forced convection in the heat transfer process which will be greater in smaller radius ratio than larger radius ratio (i.e., the cooling is greater). When the inner and outer walls approaches further together (i.e., increasing of radius ratio), The heat will be distributed in small region comparison with the smallest radius ratio (i.e., the amount of heat per unit volume will be greater). As a result, at the same rate of cooling resulting from forced convection for both cases: uniform inlet velocity and rotational velocity of the inner cylinder (i.e., Re^2/Ta), the temperature values at the same RR increase in the region of RR bounded between 0 and 0.35 as the radius ratio increases. It is noticed that, there is no temperature change in the 1st three curves (i.e., the temperature approaches t_i) in the annular gap core region toward the outer wall (RR bounded between 0.35 and 1), then the temperature values increase as radius ratio increases to 0.9 at the same RR and in the same region.

Fig.(١٩) represents the effect of radius ratio on the developing temperature profile for Gr/Re= –300 (i.e., opposing flow), Re^2/Ta=10 (i.e., very slow rotational of the inner cylinder), and at Z=0.01. It can be seen that the behavior of temperature profile trend is the same as the obtained previous profiles.

4.3 Tangential Velocity Profile

In the absence of free convection, it is Known that, provided the flow remains laminar and vortices are not generated, the rate of rotation of the inner cylinder has a slight effect on the developing tangential velocity profiles, and hence tangential boundary layer thickness. In the presence of

superimposed free convection, the present computations have also confirmed this conclusion. In other words, at a given value of Gr/Re, the parameter Re^2/Ta has a slight effect on the developing tangential velocity profiles, and hence tangential boundary layer thickness. This fact was concluded also by El-Shaarawi and Sarhan [2]. Fig.(٢٠) shows this fact which represented for N=0.555, Gr/Re=800, and at RR=0.1.

Fig.(٢١) shows the effect of radius ratio on the developing tangential velocity profile along Z-axis, for Gr/Re=500, Re^2/Ta=0.2, and at RR=1. This figure shows that the tangential velocity values increase as the radius ratio increases because of decreasing of annular gap cross-sectional area. This result will be obtained for Gr/Re= –300, RR=0.1, and Re^2/Ta=0.2 & 10; as shown in Figs.(٢٢&٢٣) respectively.

For a given value of Re^2/Ta, the parameter Gr/Re has significant effects on the developing tangential velocity profiles, and hence the tangential boundary layer thickness. Fig.(٢٤)& Fig.(٢٥) represent the developing tangential velocity (W) corresponding to a given value of the parameters, N=0.555, RR=0.1, and Re^2/Ta=1&1000, respectively, for various selected values of the parameter Gr/Re. it is noticeable from these two figures that, the superimposed aiding free convection delays the development of the tangential velocity component in comparison with the case of pure forced convection. Also, the increase in the absolute value of the parameter Gr/Re in the opposing free convection case causes an increase in the rate of tangential velocity development. There is an approaching in the values of tangential velocity downstream , and may be intersect and reverse the behavior of the tangential velocity profile if the dimensionless axial distance (Z) is greater than that given in these two figures.

This actually occurs in Figs.(٢٦ & ٢٧) which show the effect of the parameter Gr/Re on the tangential velocity development for N=0.9, Re2/Ta=10, and at RR=0.25 & 0.5 , respectively. It is clear from these two figures that , near the annulus entrance and until a certain point in the entry region, the aiding free convections delay the development of the tangential velocity component in comparison with the case of pure forced convection , then further downstream this effect is reversed. Also, in an opposing flow case, the increase in the absolute value of the parameter Gr/Re, causes an increase in the rate of tangential velocity development until a certain axial distance from the entrance is reached , after which this effect is reversed until the flow becomes fully developed.

4.4 Local Nusselt Number Nu_z

There is a very slight effect of the rotation inner cylinder on the heat transfer process. This can be seen in Fig.(٢٨) and Fig.(٢٩) which represent N=0.555, Gr/Re= –300 & 800, respectively.

Fig.(٣٠) & Fig.(٣١) show the variation of local Nusselt number (Nu_z) with the dimensionless axial distance Z for various values of radius ratio N,

Gr/Re=500, and Re^2/Ta=0.2 & 10, respectively. It can be seen that heat is removed most efficiently from the inner heated wall for small values of N because for N small the gap in the annulus would be relatively very large and even if heat is flowing into the fluid at a high rate it would be carried off downstream before it was able to penetrate very far across the gap.

The same behavior can be obtained if the flow opposes the natural convection (Gr/Re= –300), Re^2/Ta=0.2 & 10 as shown in Fig.(٣٢) & Fig.(٣٣), respectively. Fig.(٣٤) shows the effect of radius ratio on the local Nusselt number distribution for pure forced convection case (i.e., Gr/Re=0) , and Re^2/Ta=0.2. The same behavior obtained for aiding and opposing flows will be obtained in this case. On the other hand, if the parameter Re^2/Ta is fixed, there is a significant effect of the parameter Gr/Re on the heat transfer process. Fig.(٣٥) gives; for N=0.555, Re^2/Ta=1: the variation of the local Nusselt number with the dimensionless axial distance Z at various values of the parameter Gr/Re. It is clear that with positive values of Gr/Re (i.e., free convection aids the forced flow), Nu_z is higher , for the same Z, than their corresponding values of the purely forced convection case (Gr/Re=0) and vice versa with negative values of Gr/Re. This is attributed to the higher velocities near the heated surface, and hence the decrease in the thickness of the developing boundary layer on that boundary, in case of an aiding free convection. However, since the fully developed laminar velocity profile for both pure forced convection and mixed convection cases is the same as the isothermal laminar velocity profile, the mixed convection Nusselt number approaches, at large values of Z and for all values of Gr/Re, as shown in Fig.(٣٥).

It could be seen also that, at any dimensionless axial distance Z, Nu_z is very nearly a linear function of Gr/Re. This effect of free convection seen in Fig.(٣٥) decreases if the inner cylinder rotation increases (Re^2/Ta=0.2) as shown in Fig.(٣٦). This behavior can be attributed to the following fact: in the entrance region, the inner cylinder rotation causes the axial velocity boundary layer developing on the outer wall to be thickened while the inner wall axial velocity boundary layer diminishes. Thus, for aiding flow case; the values of the local Nusselt number at the same Z will be slightly increasing as Gr/Re increases and vice versa for opposing flow. The same behavior obtained in Fig.(٣٥) will be obtained in Fig.(3٧) which represent N=0.9 and Re^2/Ta=10 (i.e., slow rotational velocity). It is obvious that, with increasing the axial distance further (i.e., further downstream), the local Nusselt number approaches a fully developed value.

5. Conclusions

1. For aiding flow case , the fluid accelerates near the heated boundary and decelerates near the opposite insulated wall and vice versa for opposing flow case.

2. There is a non-significant effect of Re^2/Ta on the fluid flow and heat transfer process.

3. The thickness of the thermal boundary layer gradually increases as the flow moves from annulus inlet toward annulus exit.

4. The superimposed aiding free convection delays the development of the tangential velocity component in comparison with the case of pure forced convection and vice versa for opposing free convection.

5. For the same N, Re^2/Ta, and absolute value of Gr/Re; the heat transfer process will be better in aiding flow case than opposing flow case.

5. References

[1] M. A. I. El-Shaarawi and A. Sarhan, "Developing Laminar Free Convection In An Open Ended Vertical Annulus With A Rotating Inner Cylinder , J. Heat Transfer, pp. 552-558, Vol. 103, August , 1981.

[2] M. A. I. El-Shaarawi and A. Sarhan, "Combined Forced-Free Laminar Convection In The Entry Region Of A Vertical Annulus With A Rotating Inner Cylinder ", Int. J. Heat Mass Transfer , Vol.25, No.2 , pp.175-186 , February 1982.

[3] M. M. M. Abou-Ellail and S. M. Morcos, "Turbulent Heat Transfer In The Entrance Of A Concentric Annulus With Inner Cylinder Rotation " , Proceedings of the 7th Int. Heat Transfer Conference , München, Fed. Rep. of Germany , Vol. 3, pp. 3-8, 1982.

[4] E. Leonardi , J. A. Reizes and G. de Vahl Davis, "Heat Transfer In A Vertical Rotating Annulus- A Numerical Study " , Proceedings of the 7th Int. Heat Transfer Conference , München, Fed. Rep. of Germany ,Vol. 3 , pp. 69-74, 1982.

[5] M. A. Hessami , G. De Vahl Davis, E. Leonardi and J. A. Reizes "Mixed Convection In Vertical, Cylindrical Annuli", Int. J. Heat Mass Transfer, Vol.30, No.1 , pp. 151-164 , January , 1987.

[6] C. J. Ho, Y. H. Lin, and T. C. Chen "A Numerical Study Of Natural Convection In Concentric And Eccentric Horizontal Cylindrical Annuli With Mixed Boundary Condition " , Int. J. Heat Fluid Flow, Vol. 10, No. 1, pp. 40-47, March 1989.

[7] C. J. Ho and F. J. Tu "Laminar Mixed Convection Of Cold Water In A Vertical Annulus With A Heated Rotating Inner Cylinder " , J. Heat Transfer , Vol. 114, pp.418-424, May, 1992.

[8] Z.-Y. Guo and C.-M. Zhang "Thermal Drive In Centrifugal Fields-Mixed Convection In A Vertical Rotating Cylinder ", Int. J. Heat Mass Transfer, Vol.35, No.7, pp.1635-1644, 1992.

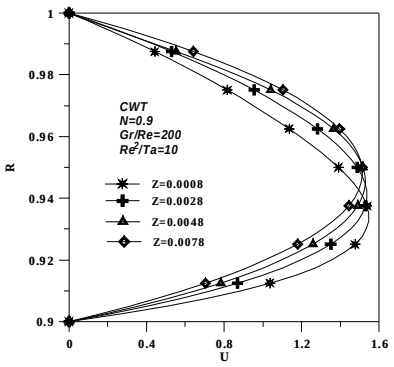

Fig.(2) Development of the axial velocity profiles along the annulus.

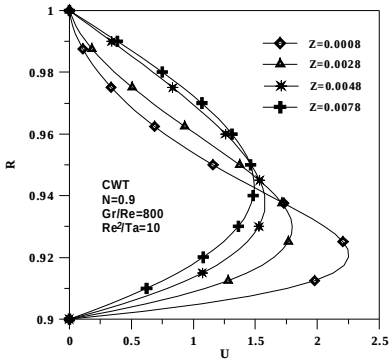

Fig.(3) Development of the axial velocity profiles along the annulus.

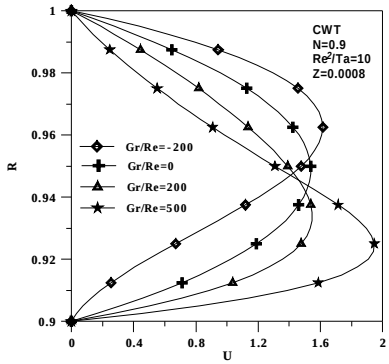

Fig.(4) Development of the axial velocity profiles along the annulus.

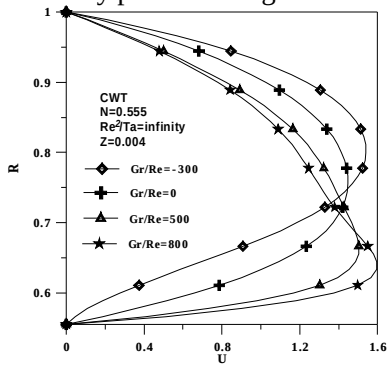

Fig.(5) Development of the axial velocity profiles along the annulus.

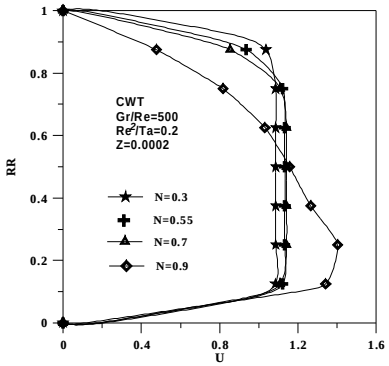

Fig.(6) Development of the axial velocity profiles along the annulus.

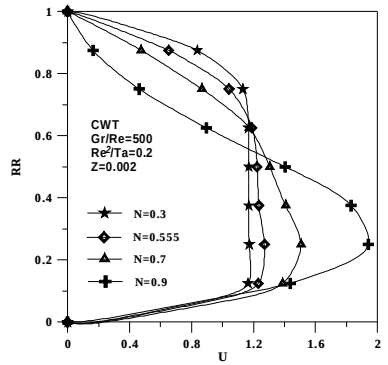

Fig.(7) Development of the axial velocity profiles along the annulus.

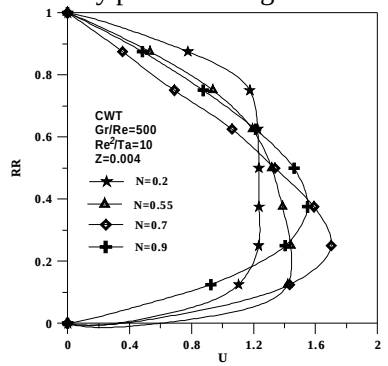

Fig.(8) Development of the axial velocity profiles along the annulus.

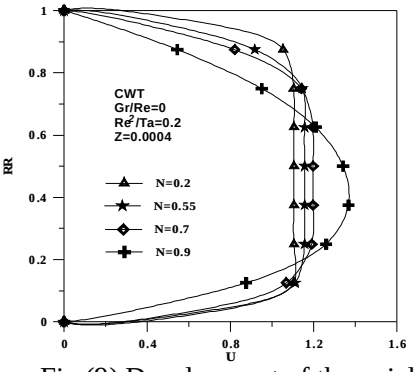

Fig.(9) Development of the axial velocity profiles along the annulus.

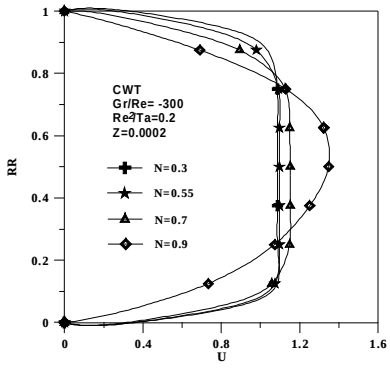

Fig.(10) Development of the axial velocity profiles along the annulus.

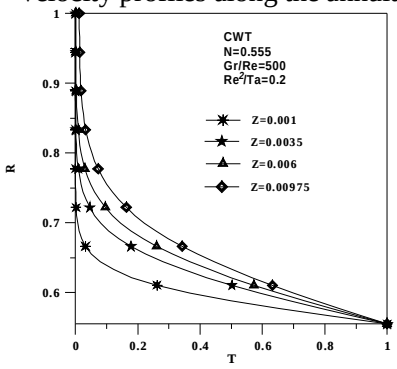

Fig.(11) Development of the temperature profiles along the annulus.

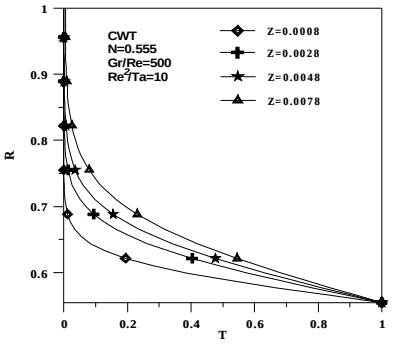

Fig.(12) Development of the temperature profiles along the annulus.

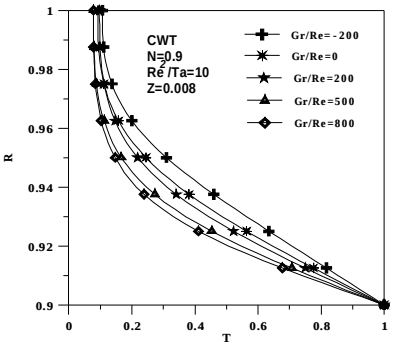

Fig.(13) Development of the temperature profiles at the same Z and various values of Gr/Re.

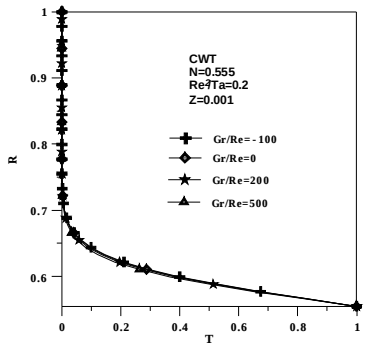

Fig.(14) Development of the temperature profiles at the same Z and various values of Gr/Re.

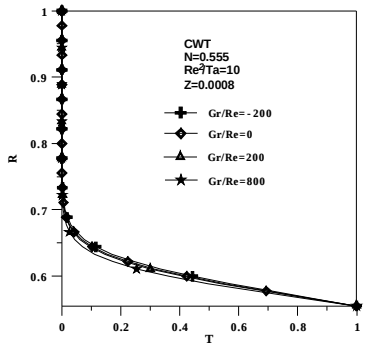

Fig.(15) Development of the temperature profiles at the same Z and various values of Gr/Re.

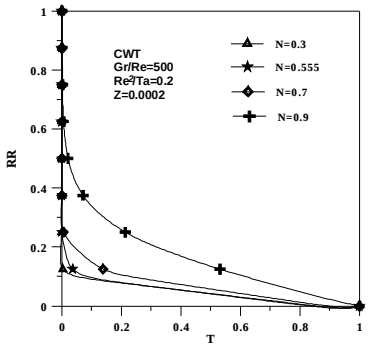

Fig.(16) Development of the temperature profiles at the same Z and various values of N.

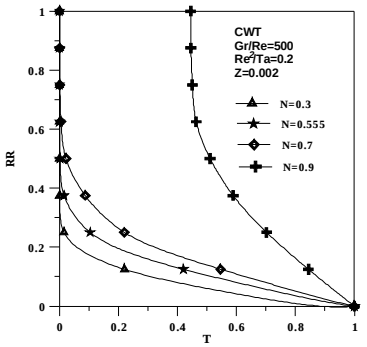

Fig.(17) Development of the temperature profiles at the same Z and various values of N.

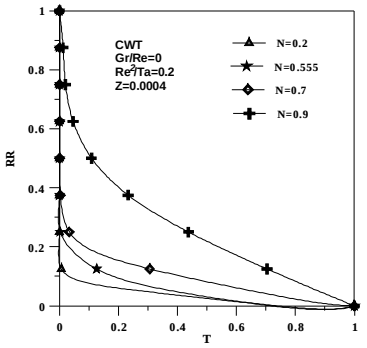

Fig.(18) Development of the temperature profiles at the same Z and various values of N.

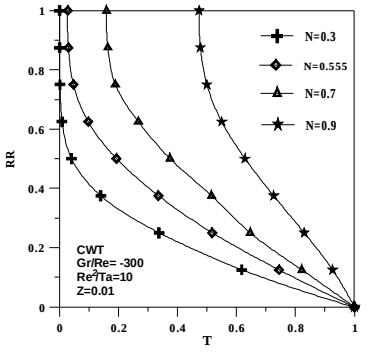

Fig.(19) Development of the temperature profiles at the same Z and various values of N.

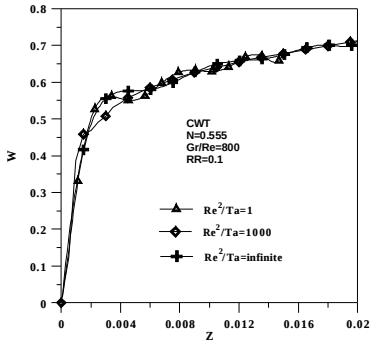

Fig.(20) Tangential velocity development along Z axis.

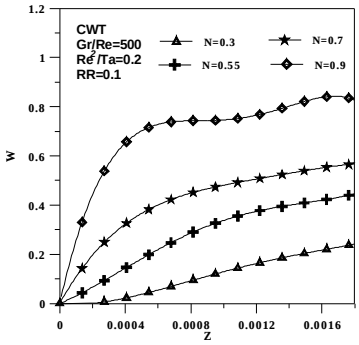

Fig.(21) Tangential velocity development along Z axis.

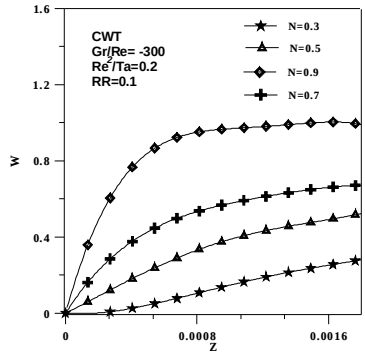

Fig.(22) Tangential velocity development along Z axis.

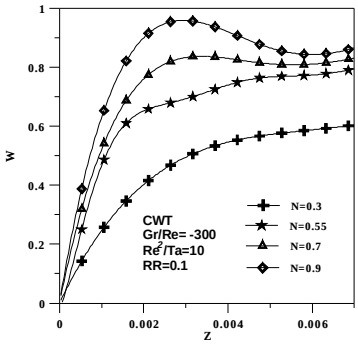

Fig.(23) Tangential velocity development along Z axis.

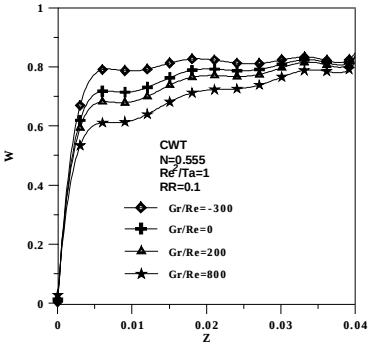

Fig.(24) Tangential velocity development along Z axis.

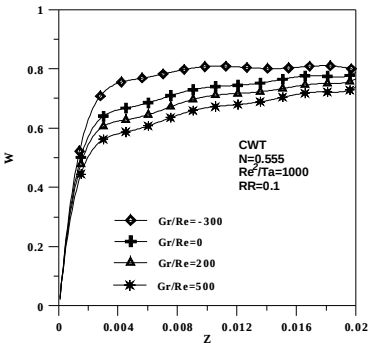

Fig.(25) Tangential velocity development along Z axis.

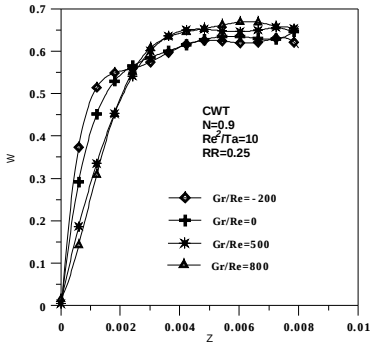

Fig.(26) Tangential velocity development along Z axis.

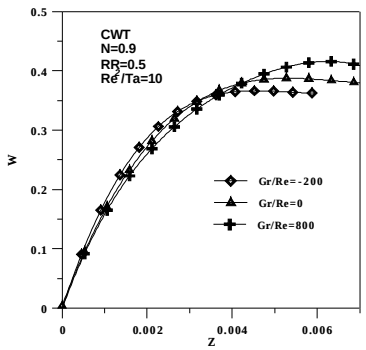

Fig.(27) Tangential velocity development along Z axis.

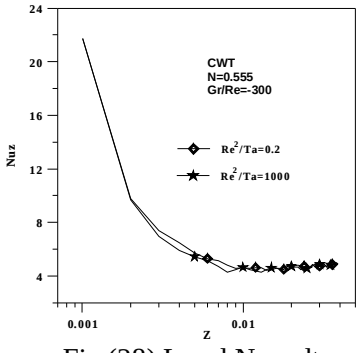

Fig.(28) Local Nusselt number versus dimensionless axial distance.

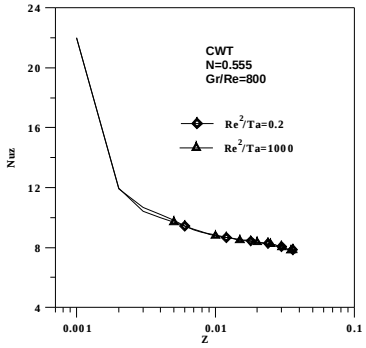

Fig.(29) Local Nusselt number versus dimensionless axial distance.

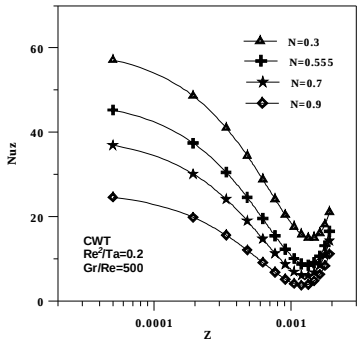

Fig.(30) Local Nusselt number versus dimensionless axial distance.

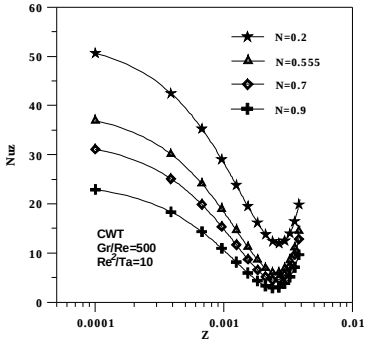

Fig.(31) Local Nusselt number versus dimensionless axial distance.

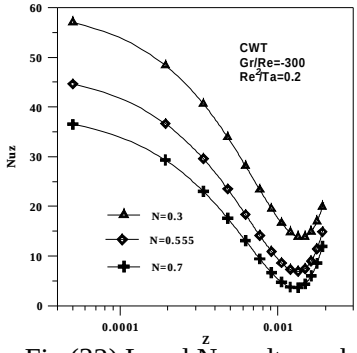

Fig.(32) Local Nusselt number versus dimensionless axial distance.

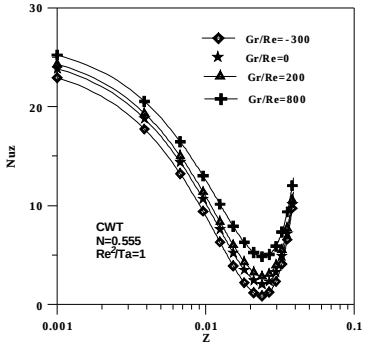

Fig.(3٥) Local Nusselt number versus dimensionless axial distance.

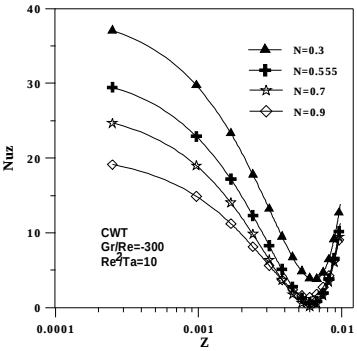

Fig.(33) Local Nusselt number versus dimensionless axial distance.

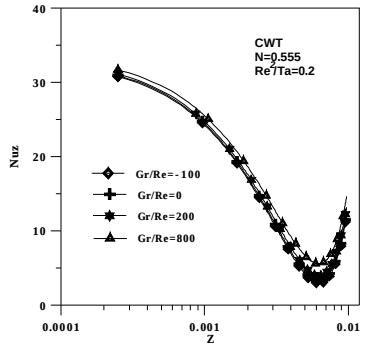

Fig.(3٦) Local Nusselt number versus dimensionless axial distance.

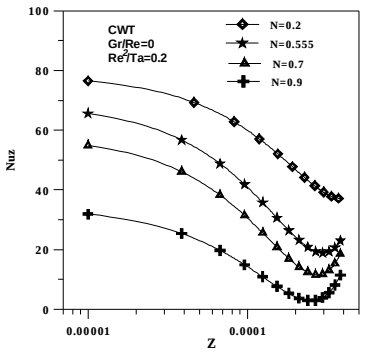

Fig.(3٤) Local Nusselt number versus dimensionless axial distance.

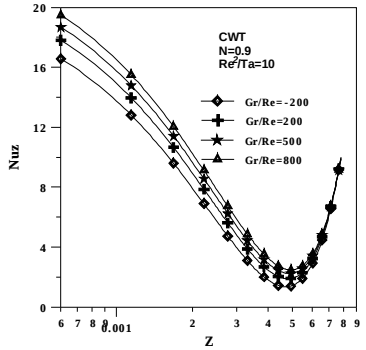

Fig.(3٧) Local Nusselt number versus dimensionless axial distance.